

# A transport of inorganic particulate matter in size-classified aerosols attached by $^7\text{Be}$ in the atmosphere in Osaka, Japan

Noithong Pannipa<sup>1\*</sup>, Hisakazu Muramatsu<sup>2</sup>, Tatsuhide Hamasaki<sup>1</sup>, Chantaraprachoom Nanthapong<sup>1</sup>, Rittirong Anawat<sup>1</sup>, and Ryuta Hazama<sup>1</sup>

<sup>1</sup>Graduate School of Human Environment, Osaka Sangyo University, 3-1-1 Nakagaito, Daito, Osaka 574-8530, Japan

<sup>2</sup>Chemistry Division, Faculty of Education, Shinshu University, 6-Ro, Nishinagano, Nagano-shi, Nagano 380-8544, Japan

\*Corresponding author's e-mail: e-mail: jaja.boky@gmail.com

**Abstract.** This study analyzed the relationship between the size distribution of  $^7\text{Be}$  aerosol particles in the surface air and major chemical composition of particulate matter (PM) in size distributions to investigate the main inorganic species of PM in atmospheric aerosol particles as a carrier of  $^7\text{Be}$ .  $^7\text{Be}$  can be used as a tracer of atmospheric pollutants. The main inorganic species of PM are nitrate ( $\text{NO}_3^-$ ), ammonium ( $\text{NH}_4^+$ ), sulfate ( $\text{SO}_4^{2-}$ ), and sea salt representing a 1:1 ratio of sodium ion ( $\text{Na}^+$ ) and chloride ion ( $\text{Cl}^-$ ). Every 2 weeks during June 6, 2020 to August 28, 2020, aerosols size distributions were collected and classified aerosol into 12 sizes ranging from 0.06 to 13.10  $\mu\text{m}$  by the low-pressure cascade impactor. The activity size distribution of  $^7\text{Be}$ -aerosols peaked in the 0.33 – 0.55  $\mu\text{m}$  size range, the activity median aerodynamic diameter (AMAD) 0.63  $\mu\text{m}$  and geometric standard deviation (GSD) 2.5. The mass size distribution of  $\text{NH}_4^+$  and  $\text{SO}_4^{2-}$  peaked in the same range as  $^7\text{Be}$  and showed MMADs were 0.61  $\mu\text{m}$ , (GSD 2.64) and 0.63  $\mu\text{m}$  (GSD 2.66), respectively.  $\text{NO}_3^-$  and sea salt showed the greater size of aerosol diameter peaked in 2.20 - 3.90  $\mu\text{m}$ , and 1.20 - 2.20  $\mu\text{m}$  size range, respectively. The dominant ionic species were  $\text{SO}_4^{2-}$  among anions and  $\text{NH}_4^+$  among cations, and their MMAD was almost identical to AMAD of the  $^7\text{Be}$  activity size distribution. For the variation of inorganic species and the variation of  $^7\text{Be}$ , we found that only  $\text{SO}_4^{2-}$  had good agreement with the variation of  $^7\text{Be}$  activity. Thus  $\text{SO}_4^{2-}$  would be the potential medium for  $^7\text{Be}$ , and this inorganic species can be traced and predicted based on the behaviour of  $^7\text{Be}$ .

**KEYWORDS:** *Beryllium-7, particulate matter, sulfate, nitrate, ammonium, and sea salt*

## 1 INTRODUCTION

$^7\text{Be}$  (half-life 53.3 d) is a natural cosmogenic radionuclide and it is continuously produced in the upper troposphere and lower stratosphere. The production of  $^7\text{Be}$  in the atmosphere is mainly due to spallation reaction between galactic cosmic ray (neutron and protons) and nitrogen and oxygen. The  $^7\text{Be}$  then become attached to aerosols and are transported to the lower atmosphere [1]. On the behavior of  $^7\text{Be}$  atoms with atmospheric aerosols, it was concluded from early aerosol studies that considerable coagulation occurred during migration of  $^7\text{Be}$  atoms from the stratosphere and upper troposphere to ground level air [2 - 4].  $^7\text{Be}$  participates in the formation and growth of the accumulation mode aerosols (0.07 to 2  $\mu\text{m}$  diameter), which is a major reservoir of pollutants in the atmosphere [5]. Following its production by gas-phase nuclear transformation, this isotope condenses on the aerosol population, growing by condensation of non-radioactive species e.g. sulfates or organic [6] and so the fate of  $^7\text{Be}$  will become the fate of the carrier aerosols [5]. The variation of  $^7\text{Be}$  concentrations in near-surface air are commonly associated with factors such as solar activity level, latitude, altitude, seasonal air mass transport, and meteorological conditions [7]. In case of particulate pollutants, since other pollutants or particulate matter (PM) are attached to aerosols,  $^7\text{Be}$  can be used as a tracer of atmospheric pollutants. The concentrations and variation of PM may alter the behaviour of  $^7\text{Be}$  in the atmosphere. It is well known that nitrate ( $\text{NO}_3^-$ ), ammonium ( $\text{NH}_4^+$ ), sulfate ( $\text{SO}_4^{2-}$ ) and sea salt representing a 1:1 ratio of sodium ion ( $\text{Na}^+$ ) and chloride ion ( $\text{Cl}^-$ ) are significant constituents of the PM [8]. Many researchers have observed the relationship between  $^7\text{Be}$  and particulate matter (PM) and note that the concentration and variation of PM can alter the behaviour of  $^7\text{Be}$  and its atmospheric distribution [7, 9]. However there have been few studies that have estimated the size distributions of atmospheric aerosols attached by  $^7\text{Be}$  and the relationship between  $^7\text{Be}$  activity and inorganic particulate matter in size distribution. Thus, the data is not clear enough. In this study, we investigated the relationship between  $^7\text{Be}$  concentration and the major chemical composition of PM in size

distribution of aerosols in order to investigate the main inorganic species of PM in atmospheric aerosol particles as a carrier of  $^7\text{Be}$

## 2 MATERIALS AND METHODS

### 2.1 Air sampling

The sampling site for aerosols' particle size distribution was at a rooftop of building No. 16, located at Osaka Sangyo University, Daito, Osaka Prefecture, Japan (34.71 °N, 135.64 °E), and approximately 31 m above ground level (AGL). Every 2 weeks from June 6, 2020, to August 28, 2020, air samples were collected using a low-pressure cascade impactor (12 stages with backup filter, Tokyo Dylec Corp., Japan, model LP-20). Aerosol sizes were classified into 12 size ranges on glass plates (80 mmΦ) for 12 stages. The point was that not a certain filter but a glass plate was used as a substrate because materials consisting of aerosol particles cannot be completely extracted from some kinds of filters. The cascade impactor was operated at a constant airflow rate of 20 L/min and 12 multi-jet stages with the cut-off values for the impactor at 50% collection efficiency of 11, 7.8, 5.2, 3.5, 2.1, 1.2, 0.7, 0.49, 0.3, 0.2, 0.12, and 0.06 μm in aerodynamic diameters.

### 2.2 Sample preparation

The air samples were extracted from the glass plate by pouring 25 ml of the ultrapure water and an ultrasonic cleaner for 15 minutes. We used 3 ml for measurement of the water-soluble inorganic ions, focused on the significant constituents of the PM are nitrate ion ( $\text{NO}_3^-$ ), ammonium ion ( $\text{NH}_4^+$ ), sulfate ion ( $\text{SO}_4^{2-}$ ), sodium ion ( $\text{Na}^+$ ), and chloride ion ( $\text{Cl}^-$ ) by ion chromatography (DIONEX, ICS-1100) and 22 ml for filtration of  $\text{Be}(\text{OH})_2$  form to measure the  $^7\text{Be}$  activity [10]. 3 ml of solution samples for ion chromatography measurement were filtered by using two types of syringe filters: 1) IC Acrodisc 13 mm (pore size 0.2 μm PES membrane, POLL), and 2) IC Maxi-Clean SPE (0.5mL IC-RP, GRACE) to protect analytical columns by removing fine particles and hydrophobic contaminants, respectively.  $^7\text{Be}$  was separated from the 22 ml sample solution by co-precipitation with non-radioactive  $\text{Be}^{2+}$  (so-called carrier). Add 0.2 ml of  $\text{BeSO}_4$  solution (1.1 mol/L) to the sample solution and several drops of pH indicator (phenolphthalein) to easily recognize the basic solution to change its color from colorless to pink. The samples were neutralized with  $\text{NH}_4\text{OH}$  solution and gave the familiar pink color.  $^7\text{Be}$  will be co-precipitated with non-radioactive  $\text{Be}^{2+}$  to form  $\text{Be}(\text{OH})_2$ . Filtrate whole  $\text{Be}(\text{OH})_2$  with a Millipore filter paper (0.45 μm pore size, 25 mmΦ). Make  $^7\text{Be}$ -sample for radioactivity measurement by covering filtrated  $\text{Be}(\text{OH})_2$  precipitation with an adhesive tape to prevent the precipitate from losing shape. It is sealed into a plastic bag to prevent the detector from radioactive contamination.

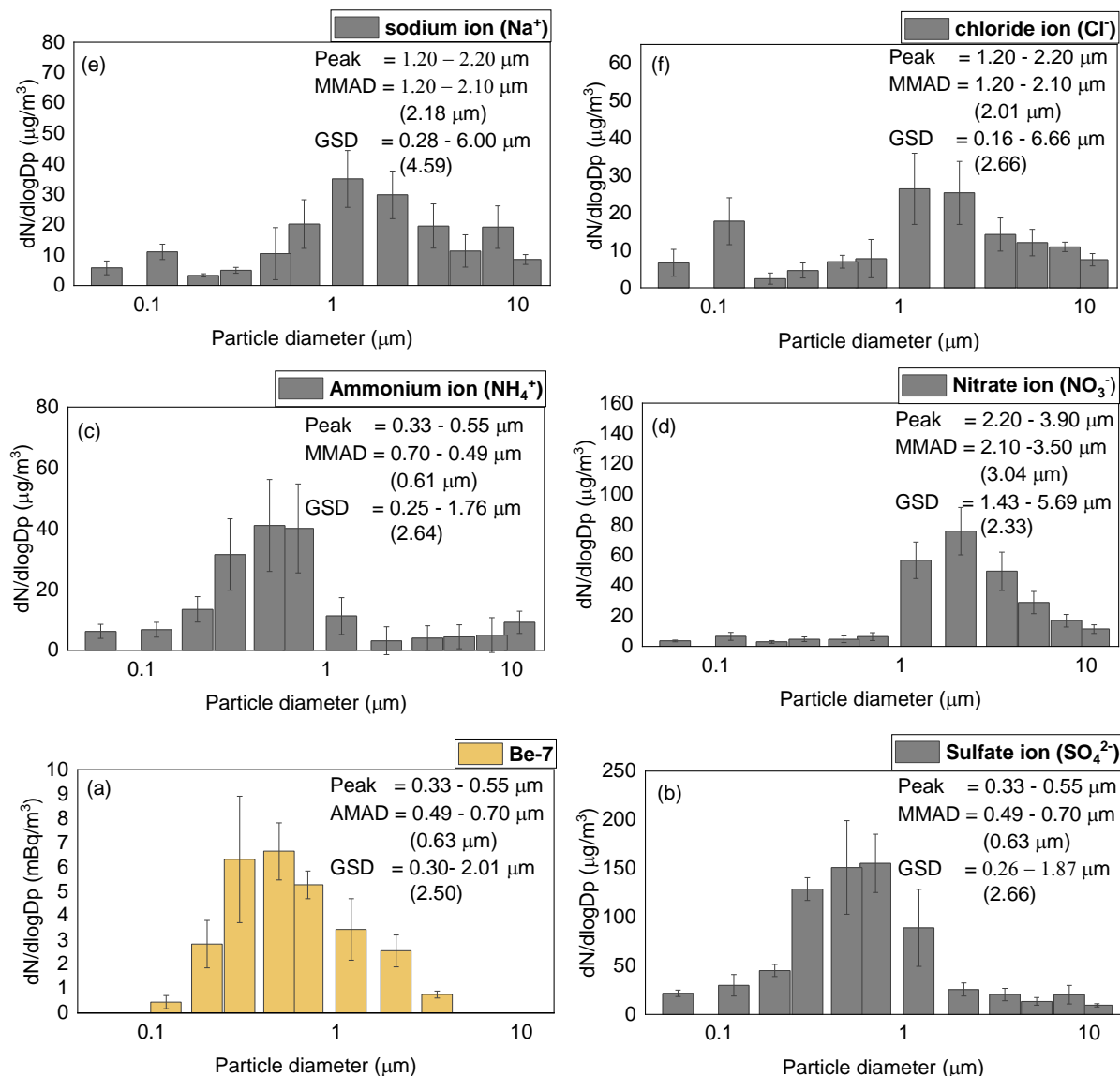
### 2.3 Measurement

3 ml of solution samples were used to analyze the concentration analyses of anions ( $\text{NO}_3^-$  and  $\text{Cl}^-$ ) and cation ( $\text{NH}_4^+$ ,  $\text{SO}_4^{2-}$ ,  $\text{Na}^+$ ) by using ion chromatography (DIONEX, ICS-1100) with a conductivity detector. The guard and the analytical column used for anion were Dionex IonPac AG14A and Dionex IonPac AS14A, respectively. The guard and the analytical column used for cation were Dionex IonPac CG12A and Dionex IonPac CS12A, respectively. The anion mixed standard solution IV and the cation mixed standard solution II (Kanto Chemical Co., INC) were used to make the calibration curve of the inorganic ions concentration. The Millipore filter paper samples were used to measure the activity concentration of  $^7\text{Be}$  by a HPGe detector (GX2018, Canberra) that was shielded with a 5-cm-thick layer of lead and 0.5-cm-thick layer of inner copper in order to reduce the background radiation. The detector was connected to a data acquisition (DAQ) system to record the gamma ray signals of 477 keV.

## 3 RESULTS AND DISCUSSION

### 3.1 Aerosol size distribution

**Figure 1:** A typical plot of the  $^7\text{Be}$  activity and inorganic ion mass size distribution versus the particle diameters



The result of the particle size distribution of inorganic  $^7\text{Be}$  and inorganic ion ( $\text{NO}_3^-$ ,  $\text{NH}_4^+$ ,  $\text{SO}_4^{2-}$ ,  $\text{Na}^+$ ,  $\text{Cl}^-$ ) (show in Fig 1). A typical plot of the activity and mass size distribution of  $^7\text{Be}$  and inorganic ion, respectively versus the particle diameters are shown. This distribution was plotted by from the average of 6 measurements, the samplings period was June 6, 2020 to August 28, 2020. AMADs were calculated from the 2-point interpolation of the data points representing the cumulative mass/activity percent above and below 50%. GSD was calculated from the 2-point interpolation of the data points representing the cumulative mass/activity percent above and below 16%. GSD has no unit because it was calculated as the square root of the ratio of the diameter at 84% the cumulative percent to 16% the cumulative percent of the mass/activity [12]. Peak is the particle diameter size range found the highest mass/activity concentration. Fig 1 (a) shows a plot of the activity size distribution of  $^7\text{Be}$  versus the particle diameter sizes. The accumulated measurement data during summer of 2020, showed the AMAD varied from 0.49 – 0.70  $\mu\text{m}$  (0.63  $\mu\text{m}$ ), and mean was 0.53  $\mu\text{m}$ . GSD calculated from 2-point of the diameter sizes were 0.30, peaked in the 0.33 – 0.55  $\mu\text{m}$  diameter sizes range, and 2.01  $\mu\text{m}$ , GSD was 2.50. In 2017, R. Matsubara et al. reported the study at Nagano, sampling site at the height 20 m AGL, and the period from May 25<sup>th</sup> to June 15<sup>th</sup>, 2016 that AMAD varied from 0.44 – 0.67  $\mu\text{m}$ , peaked in the 0.33 – 0.76  $\mu\text{m}$  diameter sizes range, and mean was 0.58  $\mu\text{m}$  [10]. Our result was in a good agreement with the result at Nagano. Atmospheric aerosol size distribution has 2 main classed with the particle sizes ranging from 0.005 – 2  $\mu\text{m}$  for fine particles and greater than 2  $\mu\text{m}$  for coarse

particles. The fine particle includes 2 size ranges: 1) Aitken nuclei, having sizes ranging from 0.005 – 0.05 and 2) accumulation particles having sizes ranging from 0.05 – 2  $\mu\text{m}$ . [12]. In 1975, Young et al. mention that in the atmosphere,  $^7\text{Be}$  is attached primarily to submicron-sized particles and report that about 88% of  $^7\text{Be}$  was found on particles smaller than 1.1  $\mu\text{m}$  in diameter [13]. In this study, the result showed that about 72.12%, 84.95 %, and 15.02% of  $^7\text{Be}$  activity was presented on particles diameter smaller than 1.1, and 2  $\mu\text{m}$  (fine particles), and greater than 2  $\mu\text{m}$  (coarse particles), respectively. In 2009, Constantin P. [14] reported the 2 year period study at Thessaloniki, Greece (40.38°N, 22.58°E) that 69% of the  $^7\text{Be}$  activity was associated with aerosol particles with diameter smaller than 1.1  $\mu\text{m}$  with AMAD 0.9  $\mu\text{m}$  (GSD = 2.24) at 20 m AGL, AMAD 0.68  $\mu\text{m}$  (GSD = 2.18) at 250 m AGL, and AMAD 0.62  $\mu\text{m}$  (GSD = 2.24) at 1000 m AGL. The  $^7\text{Be}$  activity size distribution dominated a smaller size range of particles diameter, showing a dependency on height. [14]. On particles smaller than 1.1  $\mu\text{m}$  in diameter, Constantin P (2009) [14] found the percent of  $^7\text{Be}$  activity smaller than this study and AMAD greater than this study may because of the sampling site's height lower than our sampling site. However, the important parameter associated with AMAD not only the height AGL but also depending on the relative air humidity and local weather [15]. The low humidity and high temperature in the period of this study (summer of 2020) contribute to the transport of fine particles in the air [16]. On the other hand, our result comparable with the study at Nagano reported by R. Matsubara et al. (2017) due to its study during the late of spring to early of summer Fig 1 (b) – (f) show the typical plot of the inorganic ion mass size distribution versus the particle diameters. Fig 1 (b) and (c) found the size distribution pattern of sulfate (d) and ammonium (c) ion had similar pattern and a major fraction in accumulation particle with MMAD of 0.63  $\mu\text{m}$  (GSD = 2.66) and 0.61  $\mu\text{m}$  (GSD = 2.64), respectively. Fig 1 (d) found a major fraction of nitrate ion in coarse particle with MMAD of 3.04  $\mu\text{m}$  (GSD = 2.33). Fig 1 (e) and (f) show the MMAD of sodium and chloride ion were 2.18  $\mu\text{m}$  (GSD = 4.59) and 2.01 $\mu\text{m}$  (GSD = 2.66), respectively. The mass size distribution of sulfate and ammonium ion had similar pattern with the  $^7\text{Be}$  activity size distribution. The results of this study in agreement with R. Matsubara et al (2017) who reported that dominant ionic species were sulfate ion among anions and ammonium ion among cations, and their MMAD were almost identical to the AMAD of  $^7\text{Be}$  activity size distribution [10].

**Figure 2:** the percent fraction of  $^7\text{Be}$  activity and ionic species mass below 2  $\mu\text{m}$  for fine particles and larger than 2  $\mu\text{m}$  for coarse particles.

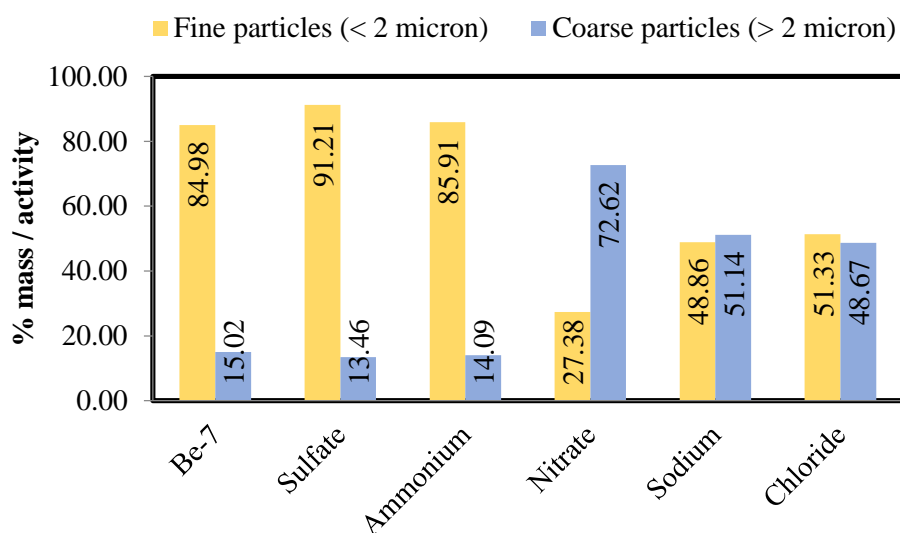


Fig 2 shows the percent of activity/mass was found in fine (<2  $\mu\text{m}$ ) and coarse (>2  $\mu\text{m}$ ) particles found that more than 80% of  $^7\text{Be}$  activity, and sulfate ion and ammonium ion mass were found in fine particles, their aerosols were principally in the fine mode in agreement with Wang et al. (2013) and Ye Tao et al. (2014) suggesting that the homogeneous gas-phase reaction between ammonia and acidic sulfate was the dominant formation mechanism of ammonium sulfate [17]. 72.62% of nitrate ion mass

was found in coarse particles, it was principally in the coarse mode, this might be explained by coarse particle nitrate ion was formed in the reaction of nitric acid with sea- and soil-derived coarse particles [18]. About 50% of sodium ion and chloride ion mass were observed both in fine and coarse particles may depended on the origins. One major source of chloride in the coarse mode particle is sea-salt, in which chloride is mainly distributed in coarse particle and is associated with sodium [19, 20]. For the fine mode, sodium and chloride ion should have another formation except the sea salt. The fine particles may come from combustion sources, including incinerators and power plants [21, 22], and secondary aerosol formation [23]

### 3.2 Variation concentration

**Figure 3:** the variation of the total activity/mass concentration

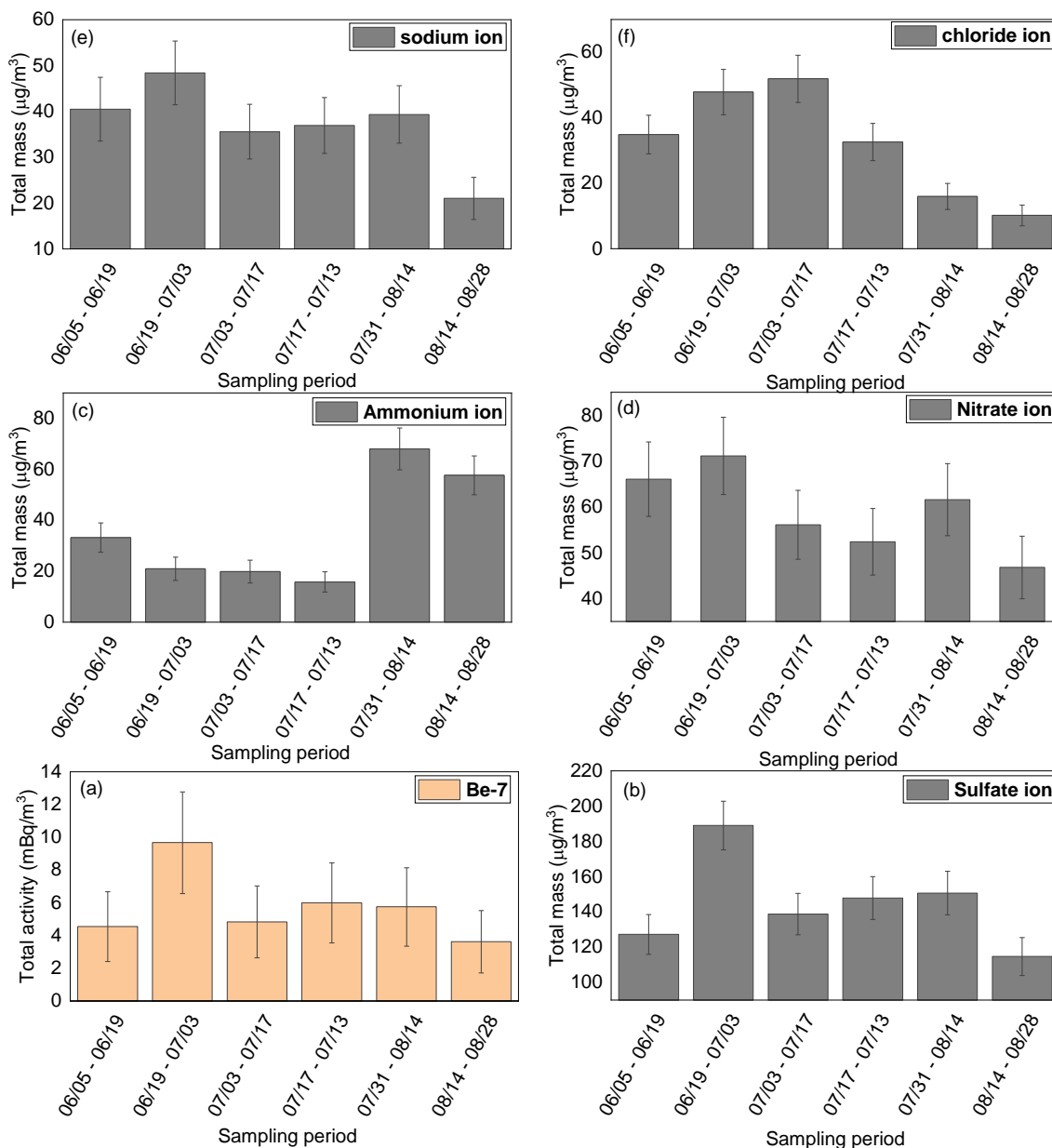


Fig 3.show biweekly <sup>7</sup>Be activity (a) and ionic species mass (b – f) concentration observed at Daito, Osaka in summer of 2020. The total <sup>7</sup>Be activity concentration ranged from 3.63 – 9.67 mBq/m<sup>3</sup>(average 1.40 mBq/m<sup>3</sup>), The comparison between the variation of the total <sup>7</sup>Be activity concentration and ionic species mass concentration found only sulfate ion that had similar pattern with <sup>7</sup>Be activity concentration. This result was different from R. Matsubara et al. (2017) reported that <sup>7</sup>Be

activity, sulfate ion, and ammonium ion mass concentration have the similar variation and seasonal pattern; it might be caused by the origin of the inorganic species, local weather and airflow origin. However, in order to confirm the result, since its airflow origin is different, the winter data is quite important. Thus, continuous measurement and analysis are required. The mass concentrations followed the sequence of sulfate ion > nitrate ion > sodium ion, chloride ion > ammonium ion. Sulfate ion found the highest mass concentration; it might be pointed out that in the area of study the major pollution came from man-made activity. Experimental data showed the sequence of sulfate ion was preponderant ions in the fine particle mode and then nitrate ion in in the coarse particle mode at all sampling periods. The sources of sulfate ion and nitrate ion not only included anthropogenic activity, but also mainly associated with the secondary pollutants formed from SO<sub>2</sub> and NO<sub>x</sub>. NH<sub>4</sub><sup>+</sup> dominated their respective mass concentrations in the fine and coarse modes, respectively. [24]

#### 4 CONCLUSION

The size distribution of <sup>7</sup>Be aerosols in near surface air overland were measurement using the low pressure cascade impactor. <sup>7</sup>Be was largely associated with the diameter particles in accumulation mode (AMAD 0.49 -0.70 μm, 0.63 μm, GSD = 2.5). This also found in sulfate ion (AMAD 0.49 -0.70 μm, 0.63 μm, GSD = 2.66) and ammonium ion (AMAD 0.49 -0.70 μm, 0.61 μm, GSD = 2.64) in agreement with R. Matsubara et al (2017). Size distribution of <sup>7</sup>Be aerosols and inorganic ionic species showed that <sup>7</sup>Be aerosol, sulfate ion, and ammonium ion dominated in fine mode particles, nitrate ion dominated in coarse mode particles and the sea salt (sodium ion and chloride ion) were comparable between coarse mode and fine modes. The comparison between the variation of the total <sup>7</sup>Be activity concentration and ionic species mass concentration found only sulfate ion that had similar pattern with <sup>7</sup>Be activity concentration. This result was difference with R. Matsubara et al (2017). The mass concentrations followed the sequence of sulfate ion > nitrate ion > sodium ion, chloride ion > ammonium ion. Experimental data showed the sequence of sulfate ion was preponderant ions in the fine particle mode and then nitrate ion in in the coarse particle mode at all sampling periods. The sources of major pollution not only included anthropogenic activity, but also mainly associated with the secondary pollutants formed. The accumulated measurement data during summer of 2020, experimental data showed the <sup>7</sup>Be activity size distribution, the percent fraction of particles size mode, and the variation concentration of <sup>7</sup>Be found only sulfate ion has good agreement with their results. Thus sulfate would be the potential medium for <sup>7</sup>Be, and this inorganic species can be traced and predicted based on the behavior of <sup>7</sup>Be.

#### 5 ACKNOWLEDGEMENTS

This work was supported by JSPS-NRCT Joint Research Program. Finally, P. N. and A. R. are supported by the Japanese Government (MEXT) Scholarship.

#### 6 REFERENCES

- [1] H. Muramatsu, S. Yoshizawa, T. Abe, T. Ishii, M. Wada, Y. Horiuchi, and R. Kanekatsu, 2008. Variation of <sup>7</sup>Be concentration in surface air at Nagano, Japan, *Journal of Radioanalytical and Nuclear Chemistry*, 275(2), pp. 299 - 307.
- [2] Friedlander, S.K., 2000. *Smoke, Dust and Haze: Fundamentals of Aerosol Dynamics*. 2<sup>nd</sup> ed. Oxford University Press, New York.
- [3] Grundel, M. and Porstendörfer, J., 2004. Differences between the Activity Size Distributions of the Different Natural Radionuclide Aerosols in Outdoor Air, *Atmospheric Environment*, 38(22), pp. 3723 – 3728.
- [4] Grundel, M., Reineking, A. and Porstendörfer, J., 2005. Activity Size Distribution in Outdoor Air: Short-lived (<sup>214</sup>Po, <sup>214</sup>Bi/<sup>214</sup>Po) and Long-lived (<sup>210</sup>Pb, <sup>210</sup>Po) Radon and Thoron (<sup>212</sup>Pb, <sup>212</sup>Po) Decay Products and <sup>7</sup>Be, *Radioactivity in the Environment*, 7, pp. 454 – 458.
- [5] Bondietti, E.A., Papastefanou, C. and Rangarajan, C., 1987. Aerodynamic Size Association of Natural Radioactivity with Ambient Aerosols. In: *Radon and its Decay Products: Occurrence,*

- Properties and Health Effects, ACS Symposium Series, 331, American Chemical Society, Washington, DC, pp. 377 - 397.
- [6] McMurry, P.H. and Wilson, J.C., 1982. Growth Laws for the Formation of Secondary Ambient Aerosols. Implications for Chemical Conversion Mechanisms. *Atmos. Environ*, 16, pp. 121 - 134.
- [7] J.H. Chao, C.C. Liu, I.C. Cho, and H. Niu, 2014. Monitoring of  $^{7}\text{Be}$  in surface air of varying  $\text{PM}_{10}$  concentrations, *Applied Radiation and Isotopes*, 89, pp. 95 – 10.
- [8] M. A. Leiva G., R. Toro, R. G. E. Morales, M. A. Ríos, and M. R. Gonzalez, 2014. A study of water-soluble inorganic ions in size-segregated aerosols in atmospheric pollution episode, *Int. J. Environ. Sci. Technol.*, 11, pp. 437 – 448.
- [9] P Noithong, A Rittirong, and R Hazama, 2019. Study of the factors influence on variation of Be-7 concentration in surface air at Osaka, Japan, *Journal of Physics: Conf. Series*, 1285.
- [10] R. Matsubara M. Hiwatashi, A. Kondo, and H. Muramatsu, 2017.  $^{7}\text{Be}$  and ionic species included in water-soluble aerosols classified by a 12-stages cascade impactor, 18<sup>th</sup> workshop on Environment Radioactivity, 9. pp. 327 - 332.
- [11] Araceli Sánchez Jiménez, Karen S Galea, and Robert J Aitken. (2011). Guidance for collection of relevant particle size distribution data of workplace aerosols Cascade Impactor Measurements. Retrieved 2020-02/09 from. <https://www.nickelconsortia.eu/assets/files/library/Guidances/IOM%20Report%202-June%202011.pdf>.
- [12] William C. Hinds, 1999. *Aerosol Technology. Properties, Behavior, and Measurement of Airborne Particles*, 2nd ed. Wiley-VCH Verlag GmbH & Co., Weinheim.
- [13] Young J.A., Tanner T.M., Thomas, C.W. Wogman, N.A. and Petersen M.R., 1975. Concentrations and Rates of Removal of Contaminants from the Atmosphere in and Downwind of St. Atmospheric Sciences, 6(5), pp. 70 - 76.
- [14] Constantin Papastefanou, 2009. Beryllium-7 Aerosols in Ambient Air, *Aerosol and Air Quality Research*, 9(2), pp. 187 - 197.
- [15] A. Mohamed, 2005. Activity size distributions of some naturally occurring radionuclides  $^{7}\text{Be}$ ,  $^{40}\text{K}$  and  $^{212}\text{Pb}$  in indoor and outdoor environments, *Applied Radiation and Isotopes*, 62, pp. 751 – 757.
- [16] Magdalena Długosz-Lisiecka and Henryk Bem, 2020. Seasonal fluctuation of activity size distribution of  $^{7}\text{Be}$ ,  $^{210}\text{Pb}$ , and  $^{210}\text{Po}$  radionuclides in urban aerosols, *Journal of Aerosol Science*, 144(105544).
- [17] Wang, L., Du, H.H., Chen, J.M., Zhang, M., Huang, X.Y., Tan, H.B., Kong, L.D., and Geng, F.H., 2013. Consecutive transport of anthropogenic air masses and dust storm plume: Two case events at Shanghai, China, *Atmospheric Research*, 127, pp. 22 – 33.
- [18] Tuomo A. Pakkanen, 1996. Study of formation of coarse particle nitrate aerosol, *Atmospheric Environment*, 30(14), pp 2475 - 2482.
- [19] Herner, J.D., Ying, Q., Aw, J., Gao, O., Chang, D.P.Y., and Kleeman, M., 2006. Dominant mechanisms that shape the airborne particle size and composition in central California. *Aerosol Sci. Technol.* 40, pp. 827 – 844.
- [20] Jinping Zhao, Fuwang Zhang, Ya Xu, and Jinsheng Chen, 2011. Characterization of water-soluble inorganic ions in size-segregated aerosols in coastal city, Xiamen, *Atmospheric Research*, 99, pp. 546 – 562.
- [21] M. A. Leiva G., R. Toro, R. G. E. Morales, M. A. Ríos, and M. R. Gonzalez, 2014. A study of water-soluble inorganic ions in size-segregated aerosols in atmospheric pollution episode, *Int. J. Environ. Sci. Technol.* 11, pp. 437 – 448.
- [22] Kaneyasu N., Yoshikado H. Sakamoto, and K. Soufuku, M., 1999. Chemical forms and sources of extremely high nitrate and chloride in winter aerosol pollution in Kanto Plain of Japan. *Atmos. Environ.*, 33, pp. 1745 – 1756.
- [23] Zhao, Y.L. and Gao, Y., 2008. Mass size distributions of water-soluble inorganic and organic ions in size-segregated aerosols over metropolitan Newark in the US east coast. *Atmos. Environ.*, 42, pp. 4063 – 4078.
- [24] Laszlo Bencs, Khaiwal Ravindra, Johan de Hoog, Elise Octavie Rasoazanany, Felix Deutsch, Nico Bleux, Patrick Berghmans, Edward Roekens, Agnieszka Krata and Rene Van Grieken, 2008. Mass and ionic composition of atmospheric fine particles over Belgium and their relation with gaseous air pollutants, *Journal of Environmental Monitoring, Journal of Environmental Monitoring*, 10, pp. 1148 – 1157.